Quasi-adiabatic calorimetry for concretes : Influential factors

Claude Boulay, Jean Michel Torrenti, Jean Luc Andre, Richard Saintilan

Quasi-adiabatic calorimetry for concretes: Influential factors

Claude BOULAY, *
Jean-Michel TORRENTI,
Jean-Luc ANDRE,
Richard SAINTILAN
Laboratoire régional des Ponts et Chaussées, Saint-Brieuc, France
Université Paris-Est, Laboratoire Central des Ponts et Chaussées, Paris, France

ABSTRACT

Quasi-adiabatic calorimetry performed on concrete specimens (known under the French acronym QAB) is a method first proposed at the LCPC Laboratory in the 1980's; it involves transposing to concrete the same procedure applied for the standardized determination of cement hydration heat (NF EN 196-9, which replaces Standard NF P 15-436). This input is essential for predicting, by numerical simulation, the thermomechanical behavior of structures. The present article offers a description of the calorimetry equipment and its performance, along with the various calculations that yield: the amount of heat released, the kinetics of this release (if the test had been adiabatic), heat flux, chemical affinity and degree of hydration. The principles behind QAB calorimeter calibration are reviewed and the magnitudes of influences assessed in order to estimate uncertainty in the heat release calculation. On the other hand, the level of dispersion inherent in the material still needs to be estimated.

Calorimétrie quasi adiabatique pour bétons : facteurs d'influence

RÉSUMÉ

La calorimétrie quasi adiabatique sur éprouvettes de béton (QAB), méthode proposée au LCPC dans les années 1980, est une transposition au béton de la procédure appliquée pour la détermination normalisée de la chaleur d'hydratation des ciments (NF EN 196-9 qui remplace la NF P 15-436). Cette donnée est essentielle pour la prédiction, par simulation numérique, du comportement thermomécanique des structures. Cet article regroupe une description du matériel et de ses performances et les différents calculs permettant d'obtenir la chaleur dégagée, la cinétique de ce dégagement de chaleur si l'essai avait été adiabatique, le flux de chaleur, l'affinité chimique et le degré d'hydratation. Les principes de l'étalonnage des calorimètres QAB est rappelé et l'examen des grandeurs d'influences permet une estimation de l'incertitude sur la chaleur dégagée. Une estimation de la dispersion inhérente au matériau serait encore à faire.

***Corresponding author:**
Claude BOULAY
claude.boulay@lcpc.fr

INTRODUCTION

Since the end of the 1980's, the development of powerful finite element computation codes has provided a glimpse into the prediction of temperature fields within massive concrete elements at an early age **[2]**. One of the data inputs, critical for this prediction, is the concrete heat of hydration. For this reason, the time was ripe for a joint LCPC - CECP-Angers project team **[3]** to develop a calorimeter labeled QAB (French acronym for "Quasi-Adiabatic for Concretes"), based on the Langavant-type semi-adiabatic calorimeters used for cement. This calorimeter and its associated testing method have since been refined given that attempts to deduce the heat release inside concrete from tests conducted on cement pastes or mortars were, [1]at the time, inconclusive.

[1]*Such tests would apparently be more feasible nowadays* ***[9]***.

The QAB test makes it possible to estimate the heat being released due to the hydration of cement contained in the concrete specimen. In knowing that all anhydrates will not be hydrated by the end of the hydration process, the heat considered herein does not allow determining the specific heat of cement hydration[2] **[20]**. On the other hand, this test incorporates all possible interactions between concrete components, including the effects of admixtures.

The QAB calorimeter is composed of a double-walled caisson (external wall made of PVC, internal wall of fiberglass-reinforced polyester) filled with an insulating material (polyurethane foam) approx. 14 cm thick **(see Fig. 1)**. The central housing of this set-up accommodates a two-part steel cylindrical shell, in which the cylindrical concrete specimen (dimension: Ø16 × 32 cm) in its cardboard mold is placed following fabrication.

figure 1
Quasi-adiabatic calorimeters used for concrete specimens (QAB).

Two identical calorimeters are used and placed in a test room held at constant temperature (20°C for a standard calorimetric test). The fresh concrete specimen is set into the first calorimeter, while a control specimen (made of concrete aged at least 3 months) is positioned in the second. It is assumed that the heat capacity of the control specimen is close to that of the test specimen. Mounanga demonstrated that a variation in this parameter with respect to hydration did exist, yet remained rather weak **[17]** (see also **[14, 15]**). Each calorimeter has been calibrated and is required to display similar characteristics. The temperature measurement chain has also been calibrated. The test then consists of recording, at regular intervals (10-15 min), the internal temperatures of both calorimeters, as well as the external temperature measured between the two calorimeters, in order to ensure room conditions are being well controlled (*see* **[6]**).

The next section will provide a review of: the equations used to transform these temperature recordings into heat released by the concrete; instrumentation employed; operating protocols for calorimeter calibration and testing; and the procedure adopted to estimate test measurement uncertainty (without incorporating reproducibility).

DETERMINATION OF HEAT RELEASED IN A QAB CALORIMETER

Let's use the following notations:

– $C_{concrete}$ [in J/°C]: heat capacity of the concrete alone; this value is calculated from concrete composition and specimen mass m_S measured after fabrication,

[2]*The specific heat of cement hydration is the quantity of heat per unit mass (in J/g) required for complete hydration.*

– C_{alu} [J/°C]: heat capacity of the reference cylinder introduced to characterize the calorimeter during its calibration procedure,
– C_{cal} [J/°C]: heat capacity of the calorimeter, as output from the calibration step,
– C_{tot} [J/K]: total heat capacity = $C_{concrete} + C_{cal}$ during a test on concrete, or = $C_{alu} + C_{cal}$ during calorimeter calibration,
– E_a [J mol^{-1}]: activation energy,
– R: perfect gas constant [8.314 J mol^{-1} K^{-1}],
– t [hours]: time elapsed during the QAB test,
– t_{cor} [hours]: corrected thermo-activation time,
– $T_{concrete,}$ [K]: temperature of the fresh concrete specimen
– T_{ext} [K]: exterior temperature to ensure controlled test room conditions,
– $T_{control}$ [K]: temperature of the hardened concrete control specimen. The control specimen is placed inside a QAB calorimeter identical to that containing the fresh concrete specimen. The value of this temperature is close to ambient temperature and evolves with fluctuations in ambient temperature, according to a time constant nearly equal to that found for the fresh concrete specimen temperature,
– $q(t)$ [J]: heat release at time t,
– $\theta(t)$ [°C] = $T_{concrete} - T_{control}$: deviation in temperature between the fresh concrete specimen and the hardened concrete control specimen at time t,
– T_{adia} [K]: heating of concrete under adiabatic conditions,
– α [J/h/°C]: heat conduction coefficient, which depends on the deviation between temperature at the core of the active calorimeter and control calorimeter temperature according to the expression $\alpha = a + b\,\theta$, where coefficients a and b are obtained through calibration.

In the QAB calorimeter, part of the heat released due to cement hydration increases the specimen temperature while another part increases the calorimeter temperature, and the remainder gets discharged to the outside. For the QAB calorimeter, these effects are expressed as follows:

$$q(t) = C_{tot}\left(\theta\ (t) - \theta\ (0)\right) + \int_0^t (a + b\ \theta(u))\ \theta(u)\ \mathrm{d}u \qquad (1)$$

This equation is derived by first writing the heat balance for both the calorimeter containing the sample and the calorimeter containing the control specimen, and then by combining the two resulting equations. This procedure allows skirting the complex task of having to measure ambient temperature by assuming that the cooling speeds of the two calorimeters are equivalent, a condition that may be reflected by:

$$\frac{C_{tot}(\text{control})}{\alpha_{control}} = \frac{C_{tot}(\text{test})}{\alpha_{test}} \qquad (2)$$

$C_{tot}(\text{control})$ and $C_{tot}(\text{test})$ are roughly equal since the control set-up contains a specimen composed of the same pre-hardened concrete and since the two calorimeters have been developed using the same technology (with nearly equal heat capacities when empty and very similar heat loss coefficients). Nonetheless, given that α depends on temperature, this hypothesis cannot hold throughout the test duration. The only way to overcome this obstacle would be to regulate ambient temperature and then ensure that the initial control temperature is close to this regulated temperature (*see* **[10]**)

The expression for $q(t)$ constitutes the test result. **Figure 16** offers a glimpse of such a result for a conventional concrete whose mix design components are listed in **Table 2**.

Additional calculations become feasible once the quantity of heat released has been determined. Since the heat capacity of concrete is known, it is possible for example to calculate **[3]** the temperature rise in this specimen should it have been placed under adiabatic conditions, i.e.:

$$T_{adia}(t) = T_{béton}(0) + \frac{q(t)}{C_{béton}} \qquad (3)$$

The association between T_{adia} and t in this initial correction cannot be assigned any real meaning; had the test actually been adiabatic, then thermo-activation of the cement hydration reaction would have accelerated the heat release over time **[3, 10]**. In this case, a second correction would need to be applied on the time parameter, by applying Arrhenius' Law in order to introduce activation energy E_a.

This corrected time is then given by the following expression:

$$t_{cor}(t) = \int_0^t \left[e^{\left(\frac{E_a}{RT_{adia}(u)} \right)} - e^{\left(\frac{E_a}{RT_{concrete}(u)} \right)} \right] du \qquad (4)$$

The determination of activation energy E_a (in J/mol) has been discussed in the technical manual entitled "Concrete strength in structures: Maturity measurements" **[13]**. Note: R is the perfect gas constant (i.e. equal to 8.314 J mol^{-1} K^{-1})

Calculation of the two previous relations produces **(Fig. 2)** the curve T_{adia}, (t_{cor}), which ultimately yields the adiabatic evolution in concrete temperature.

Figure 2
Derivatioin of the temperature curve under adiabatic conditions.

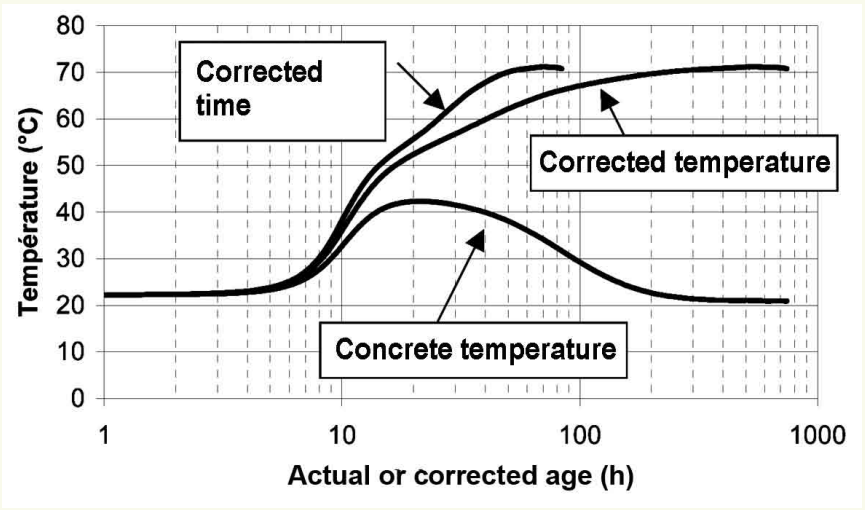

This analysis of semi-adiabatic test results on concrete, cement or mortar does not generate an evolution exactly identical to the results of an adiabatic test **[10, 12]**. For one thing, these corrections undoubtedly introduce deviations, though the authors emphasize that chemical species formed at one temperature may differ from those formed at other temperatures.

Heat flux proves straightforward to determine, except for the difficulties inherent when evaluating a slope based on experimental data, which always seem to contain noise. Data noise can be reduced by various conventional techniques (analog or digital filtering, etc.).

With respect to the same mix design presented in **Table 2**, this determination is depicted **(Fig. 3)** in the form of two calculations. The first slope evaluation of the $q(t)$ curve focuses on two successive points, and this calculation is associated with a noise. The second calculation includes 6 points on both sides of the central point (± 30 min until reaching a time of 29 h and ± 6 h beyond). Under these conditions, smoothing of the second calculation turns out to be entirely satisfactory, as the peak height remains unchanged and no temporal offset is introduced. For concretes with fast kinetics, it would most certainly be necessary to alter the search interval in order to narrow the smoothing time window.

For this numerical processing step, it is preferable to utilize a regular measurement interval (e.g. 10-15 min), but this was not the case for the test presented herein.

Figure 3
Heat flux obtained by numerical derivation of the heat release curve.

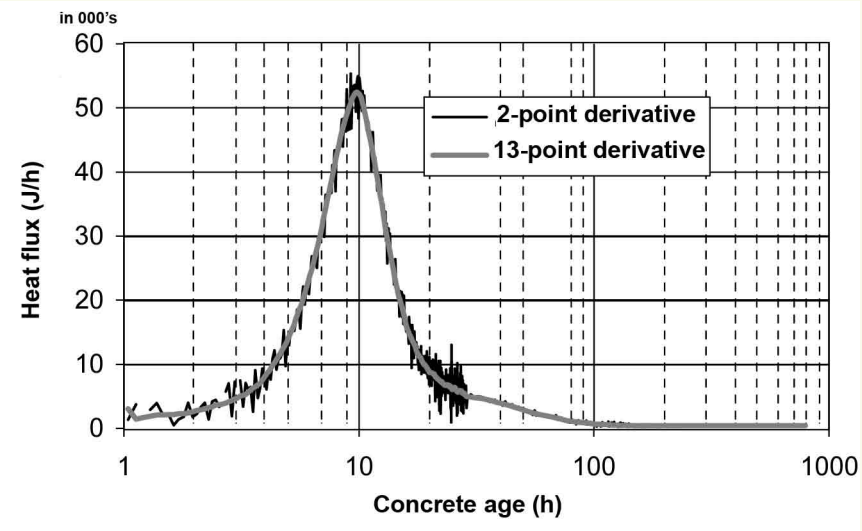

Another tool employed during these calculations to estimate changes in both the degree of hydration and rate of heat release vs. temperature history is chemical affinity.

The variation rate in degree of hydration, denoted $\xi(t)$, can be expressed as a function of chemical affinity $\tilde{A}(\xi)$ along with a term expressing thermo-activation **[18]**, i.e.:

$$\frac{d\xi}{dt} = \tilde{A}(\xi)\exp\left(\frac{-E_a}{RT}\right) = \frac{dq}{dt}\frac{\xi_\infty}{q_\infty} \quad (5)$$

where ξ_∞ is the final degree of hydration and q_∞ the final amount of heat released.

Chemical affinity can then be written as follows:

$$\tilde{A}(\xi) = \frac{d\xi}{dt}\exp\left(\frac{E_a}{RT}\right) = \frac{d\xi}{dt_{eq}}\exp\left(\frac{E_a}{RT_0}\right) \quad (6)$$

Time t_{eq} is the equivalent time required to reach, at constant temperature T_0, the degree of hydration obtained (in real time) after any temperature history profile.

The degree of hydration $\xi(t)$ corresponds to the ratio of the quantity of cement that has entered into reaction to the initial quantity of anhydrates. This degree of hydration does not necessarily reach a value of 1 once hydration has stopped, but instead a value ξ_∞. A number of models are available in the literature to estimate this value. As an example, Waller **[20]** proposed, based on a collection of results from the literature and his own research, an expression adapted to CEM I-type cements related to the water/cement (w/c) ratio as follows:

$$\xi_\infty = 1 - \exp(-3{,}25\ \frac{e}{c}) \quad (7)$$

The degree of hydration is also expressed as a function of the degree of reaction progress, denoted here as $\gamma(t)$, according to the equations:

$$\xi(t) = \gamma(t)\ \xi_\infty \qquad \text{with:} \qquad \gamma(t) = \frac{q(t)}{q_\infty} \quad (8) \text{ and } (9)$$

$$\text{which leads to: } \frac{\xi(t)}{\xi_\infty} = \frac{q(t)}{q_\infty} \quad (10)$$

A good estimation of the final value q_∞ of $q(t)$ can then be produced should the semi-adiabatic test be extended for a long enough period of time **[6]**.

Figure 4 shows the chemical affinity deduced from a calorimetric test conducted on the concrete described in **Table 2**.

Figure 4
Chemical affinity smoothed using a mathematical model [16]

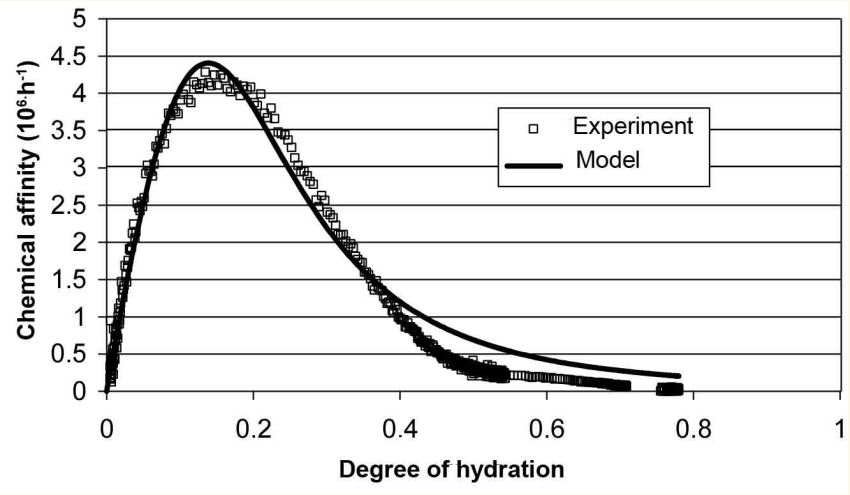

These points, which stem from experimental results, can then be represented by a mathematical function in order to perform numerical calculations. As an illustration, the model $\tilde{A}(\xi) = c_1 \frac{1-\exp(-c_2\ \xi)}{1\ +\ c_3\ \xi^{c_4}}$ proposed by Lackner *et al.* **[16]** is perfectly well suited. Coefficients c_1 through c_4 of this model are adjusted according the least squares method. A high-degree polynomial adjusted in a similar manner could also be used in this case **[8]**.

TESTING INSTRUMENTATION

Description of the calorimeter

The calorimeter is composed of a PVC box insulated using polyurethane foam. The specimen housing, located at the center of the caisson, has been designed for placement inside an intermediate steel cylinder 1.5 mm thick. An insulated cover provides access for the cable connecting the temperature probe, which has been set into a sealed copper tube placed at the base and filled with oil **(Fig. 5)**.

To ensure adequate test reproducibility, the thicknesses of polyurethane foam insulating layers must match as closely as possible. As an order of magnitude, this insulating thickness is sufficient to maintain, in the steady state, a temperature of 35°C (i.e. above a 20°C ambient temperature) for a 3.5 W internal heat source.

Rubber type joints provide the necessary seal. The calorimeter bases are essential for ventilation beneath the caisson, so that wall temperature of the device is actually being dictated by the ambient air. Without this precaution, the heat loss coefficient derived by calibration might have to be modified. It has even been recommended to install the caisson on a table at a height that allows for stirring on the under-surface yet low enough to easily place the specimen inside the caisson (i.e. at a height of approx. 40 cm).

The control calorimeter

To conduct a test, two calorimeters are introduced. A control specimen is positioned inside a QAB calorimeter (shown as no. 6 here) that matches the calorimeter receiving the fresh concrete specimen (no. 5). Control specimen temperature is close to ambient temperature and evolves with fluctuations in ambient temperature using nearly the same time constant as for the fresh concrete specimen temperature. The following experiment yielded an estimation of time constants for the two matching calorimeters. In order to test for the delayed effect in comparison with external temperature variations, two concrete cylinders aged at least 3 months were placed in the calorimeters and their temperature was recorded throughout the test duration. Room temperature was initially set at

Figure 5
Cross-section diagram of the QAB calorimeter (actual proportions are shown).

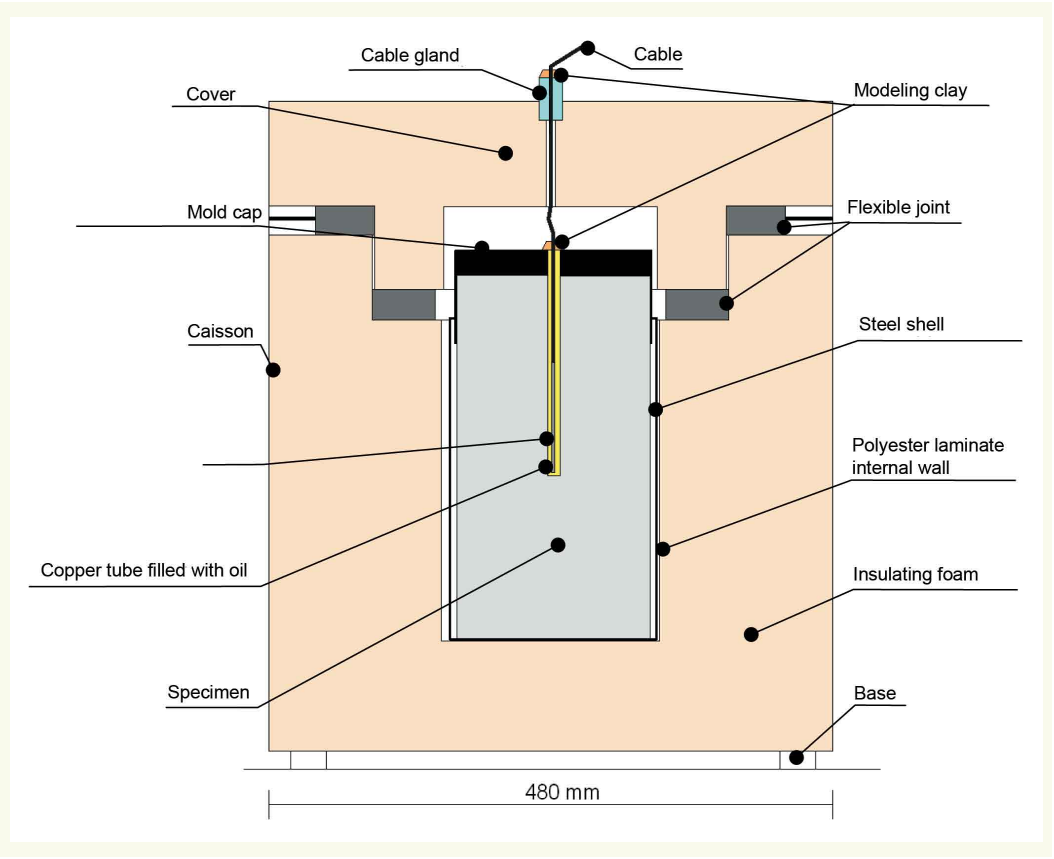

16°C, and temperature stabilization was anticipated. A recommended temperature of 26°C was then applied; the rise in room temperature from 16° to 26°C took 2.5 hours.

It can be seen that in 2 days' time, the concrete specimens only increased in temperature to 21.5°C. These recordings were nearly identical in both calorimeters **(Fig. 6)**.

In order to quantify the differences in thermal behavior between the two calorimeters subjected to this external temperature loading, a numerical simulation was implemented; this simulation consisted of calculating, according to a step-by-step procedure, internal temperature as a function of the previous time step (a numerical resolution of systems of differential equations using Euler's method). Just a single parameter, i.e. the time constant, underwent adjustment, as based on a set of recorded points (see **Fig. 6**, from 0 to 44 hours). The time constant τ_5 of Calorimeter 5 equals 55.7 h, while that of Calorimeter 6 (τ_6) is 53 h. At this stage, it can be affirmed by observation that the time constants corresponding to these two different calorimeters differ by no more than 5%.

Figure 6
Internal temperature recordings of both calorimeters in response to temperature level inside the test room.

Figure 7
Imposed temperature level outside the calorimeters, internal responses and model indicating long-term extrapolation.

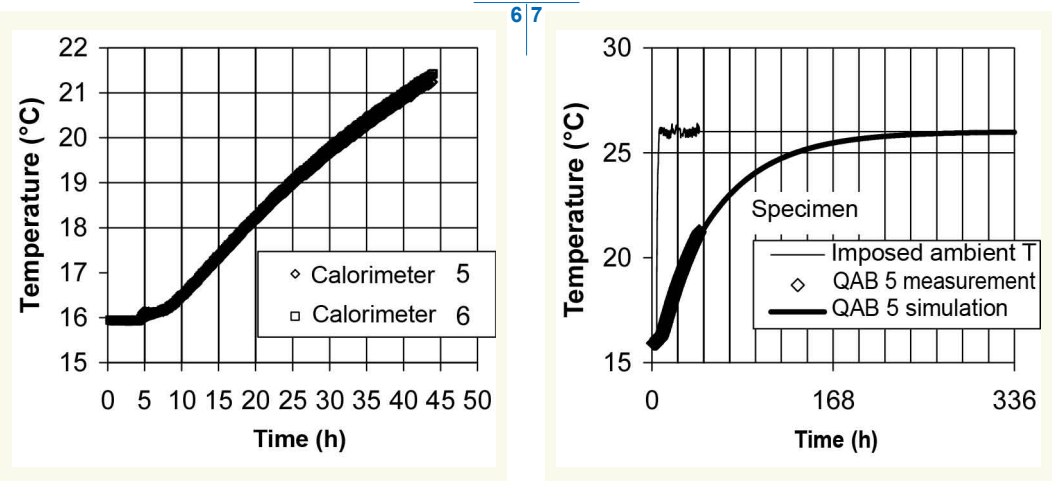

Let's recall that the curve can then be extrapolated out to two weeks .**(Fig. 7)**. 273 hours are required for the internal temperature to reach 99% of the level imposed on the outside, equivalent to 5 times the time constant value

What is the impact on the measurement of θ from such a deviation in time constants? The modeling approach adopted offers an answer to this question by replacing external temperature by dummy fluctuations (that are still realistic) of a test room over a two-week period. Fluctuations with a 20-min period and 1°C amplitude were applied and assumed to represent temperature variations due to test room regulation. These fluctuations were then superimposed by daily 1°C fluctuations, assumed to simulate the *daytime/nighttime* alternation often found in test rooms. This scenario was then repeated for two weeks **(Fig. 8)**.

8 | 9

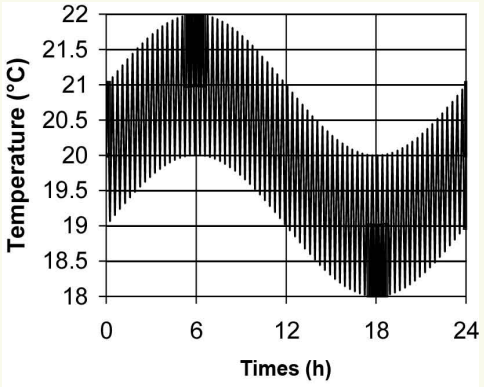

Figure 8
Ambient temperature imposed at the start of the simulation, on a 24-hour mesh - this pattern is repeated 14 times.

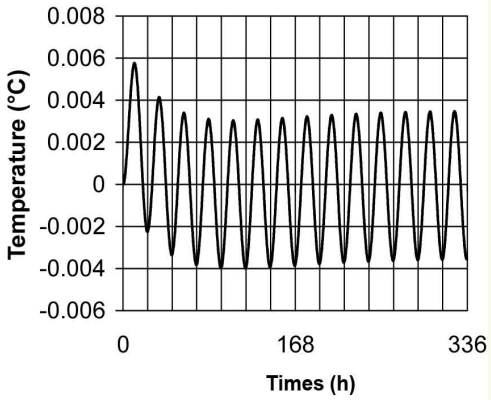

Figure 9
Evolution in temperature deviation between the two calorimeters when their time constants are same as those of the studied calorimeters.

Figure 9 shows the trend in temperature deviation for the time constants previously determined (their ratio τ_5/τ_6 equals 1.051). This set of points is considered to be a population of temperature deviations between the two calorimeters as ambient temperature fluctuates; this population can be characterized by its standard deviation.

The next step is intended to observe how this standard deviation evolves with respect to the ratio τ_5/τ_6 by varying just τ_5 in a way that allows spanning the 0.8-1.2 interval. The tracking of 2 times this standard deviation (which is considered the standard uncertainty with an expansion factor of 2) is displayed in **Figure 10**.

It is observed that when the time constant of one of the calorimeters deviates by 20% in either direction from the other calorimeter constant, the expanded uncertainty ($k = 2$) remains less than 0.025°C. For the calorimeters studied herein (whose time constants differ by 5%), expanded uncertainty is estimated at 0.005°C. As will be discussed at greater length in the section devoted

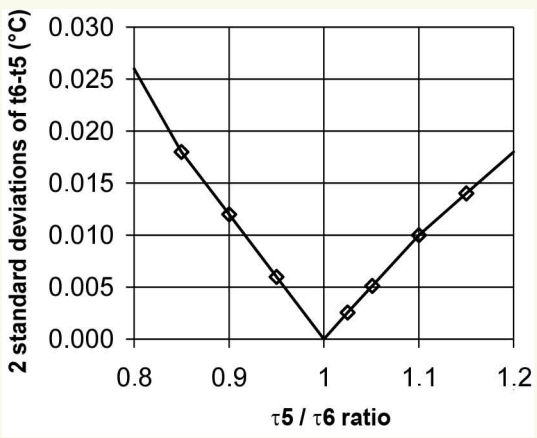

Figure 10
Expanded uncertainty on temperature deviation between the two calorimeters when their time constants vary with respect to one another. This estimation is conducted for an ambient temperature fluctuation of plus or minus 2°C around the 20°C threshold.

uncertainties, it can already be concluded, with inspiration from the findings drawn by Mounanga **[17]**, that the influence of variations in ambient temperature on the accuracy of temperature deviation between the two calorimeters is negligible given that such variations remain relatively mild.

Temperature probes

The temperature probes to be used contain platinum resistors (100 Ω at 0°C); they need to be cabled according to the Kelvin method (4 connection wires leading to the signal conditioner, 2 for the constant current power supply and the other 2 for voltage readings at the resistance terminals). If probe responses between 0° and 100°C were assimilated to a straight line, then the error committed would be that shown in **Fig. 11**.

figure 11
Écarts, en °C, entre les points d'une table pour sonde de platine et sa réponse linéaire entre 0 et 100 °C.

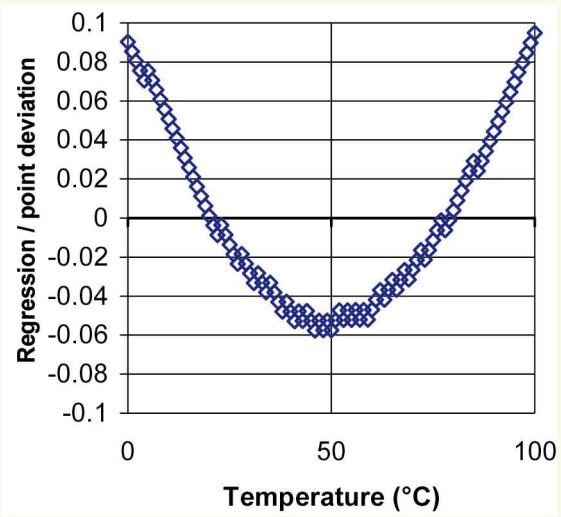

Even though this error is quite small, the level of accuracy can still be improved by applying a correction. The resistance between 0 and 100°C is, according to ITS-90 (i.e. International Temperature Standard - 90), given by the following equation:

$$R_T = R_0(1 + A\,T + B\,T^2) \qquad (11)$$

where R_T (Ω) is resistance of the platinum probe at temperature T (°C).

The coefficients A, B and R_0 are found by calibration, with nominal values of: $A = 3.9083\ 10^{-3}$, $B = -5.775\ 10^{-7}$, and $R_0 = 100$ Ω (which is the resistance value at 0°C).

The practical problem to be solved here is the inverse, i.e. to calculate temperature once resistance is known (after being deduced from voltage and current measurements). In this case, the practical function becomes:

$$T = -245.66 + 2.3556\,R_T + 0.0010115\,R_T^2 \qquad (12)$$

with R_T expressed in Ω and T in °C.

The probes are placed at the specimen core in a copper tube Ø8 mm inside and 10 mm outside, with an opening towards the bottom and a lip (flared nipple) on top. This tube crosses the flexible cap (after cutting out a hole at the center) that is sold with the packaged molds. Once the specimen has been positioned inside the calorimeter, the probe is slid into the tube and paraffin oil is poured until the tube is entirely filled. Measurement resolution must be at least 0.01°C. It is possible to reach an expanded uncertainty of 0.17°C over the full calibration chain, in which case the standard uncertainty can be rounded to 0.1°C.

Despite the strong recommendation to only supply these platinum probes during the actual measurement phase (so as to avoid self-heating, which could be detrimental to probe accuracy), the question can still be raised whether a continuously-supplied probe leads to a heat release that interferes with a precise reading of specimen heat release. The heat dissipated by means of the Joule effect during a test on concrete is not completely offset when using a set-up with both an active calorimeter and a control calorimeter. The excess heat in the active calorimeter stems from the phenomenon of its platinum resistance value not following the same trend as that of the control calorimeter. This excess is given by the expression:

$$q_j(t) = I^2 \int_0^t (R_{TA}(t) - R_{TT}(t))\, dt \qquad (13)$$

where $R_{TA}(t)$ and $R_{TT}(t)$ are probe resistances of the active and control specimens, respectively. The currents circulating in the two probes are assumed to be equal. On an actual test (using the **Table 2** mix design), the calculation (in **Table 1**) is performed for a current varying from 1 to 10 mA. Let's note that this choice of current is not without consequences.

Table 1
Excess heat released by the Joule effect, at 4 weeks into the test period in the active calorimeter and with the platinum probes being continuously supplied

Current (mA)	1	2	3	4	5	6	7	8	9	10
Heat release (J)	248	991	2,229	3,963	6,192	8,916	12,136	15,851	20,061	24,767

Figure 12 shows the evolution in heat release for the two extreme currents over the fixed interval.

Figure 13 indicates the relative error (for a total heat release in concrete of 725,600 Joules) committed on the heat release measurement vs. supply current. In conclusion, it is preferable (if possible) to select a 1 mA current, as this leads to a relative error for the concrete of just 0.03%, which depends on total heat released by the cement. For cements with a low heat of hydration, it is also preferable to select a supply current on the order of 1 mA. For CEM I (which applies to the present study), the supply current should not exceed 3 mA (with a dissipated power of 0.9 mW at 0°C and 1.25 mW at 100°C).

Another approach to this same problem consists of acknowledging the heat release and subtracting it from the result derived in Equation 1. Under these conditions, only the temperature accuracy criterion (self-heating of the probe by means of the Joule effect) is to be taken into account.

Figure 12
Excess heat released by the Joule effect in platinum probes. The differential impact of measurements using two calorimeters does not fully compensate for this effect, since temperature histories for the two calorimeters differ.

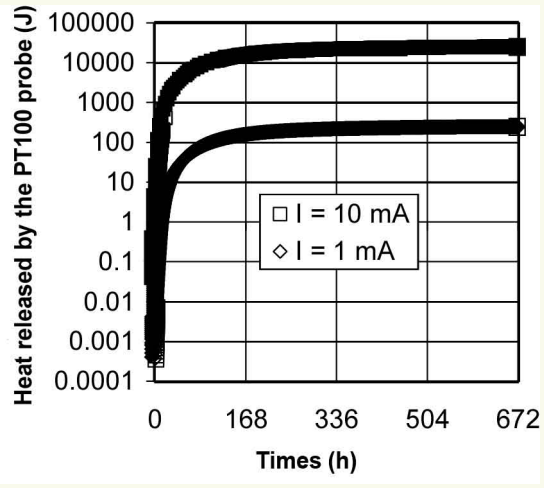

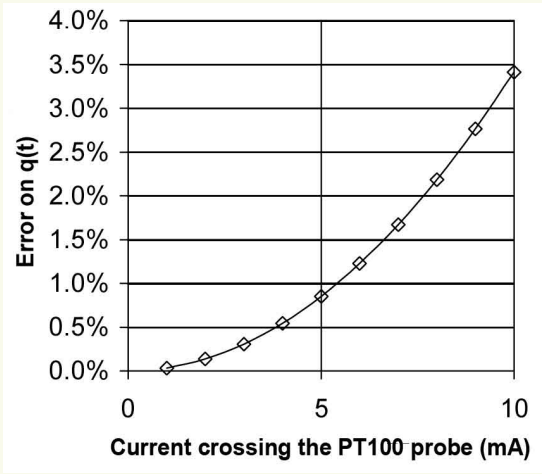

Figure 13
Percentage of error committed on the estimation of heat released by concrete vs. continuously-applied platinum probe supply current (calculation conducted for the concrete described in Table 2).

CALORIMETER CALIBRATION

The calibration procedure for QAB calorimeters involves determining both the heat loss coefficient α, which is a linear function of temperature θ (with *b* and *a* being the corresponding linear coefficients), and the heat capacity C_{cal} of the calorimeter **[1]**.

Determination of heat loss coefficient

Determining the heat loss coefficient entails positioning an aluminum cylinder fitted with a heating resistance inside the calorimeter to be calibrated, alongside a matching control calorimeter containing an identical cylinder that has not been equipped with a resistance. Temperatures are recorded at the core of both cylinders (θ denotes the difference in temperature between the two calorimeters). In the vicinity of the calorimeters, the average temperature must lie between 19 and 21°C (monitored is required using an external probe), with fluctuations around this average not to surpass ±0.5°C. Air inside the test room must be regularly circulated. Voltage at the resistance terminals along with the circulating current are measured whenever the temperature reaches a plateau, at which point the energy dissipated by the Joule effect ($P = U\,I = R\,I^2$) has been completely channeled to the outside.

In analyzing calorimeter calibration data (4 temperature plateaus), the existence of an apparent linear relation is readily observed **(Fig. 14)** between the power emitted by the Joule effect and the temperature deviation between the reference cylinder and the control cylinder. For the calorimeter targeted herein, the slope of this linear relation equals 369.8 J/h/°C.

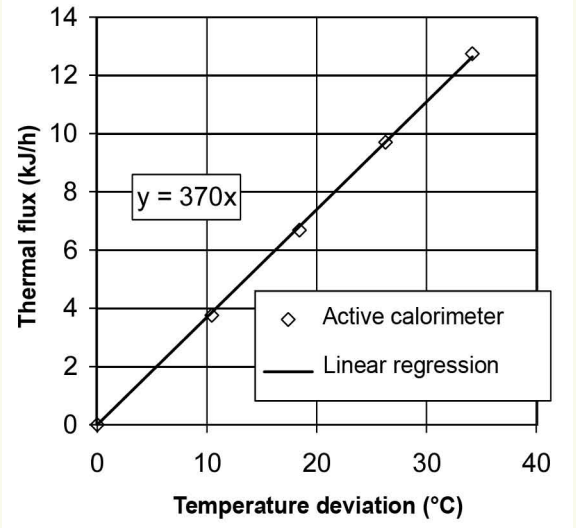

Figure 14
The heat (loss) flux through the QAB calorimeter sidewalls appears to be proportional to the temperature deviation between the reference cylinder and the control cylinder. The linear regression is forced at the point 0,0 (i.e. zero temperature deviation = zero flux).

Figure 15
Graph of the nonlinearity existing in heat flux vs. temperature deviation between the reference cylinder and the control cylinder. Flux deviations between measurement points and the regression line are depicted on this graph.

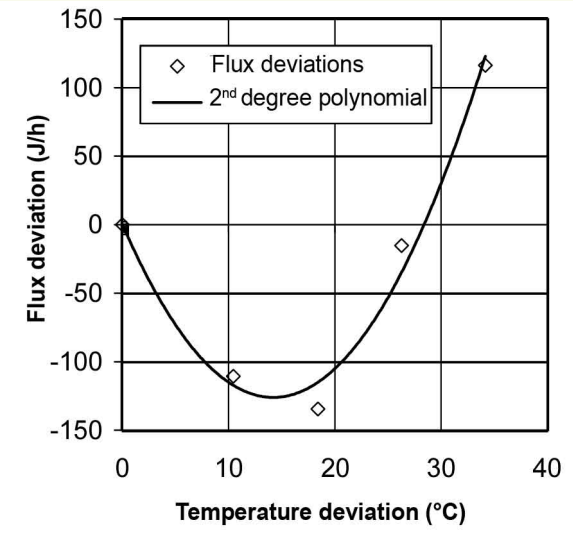

As an initial approximation, these findings reveal that the heat loss coefficient (i.e. the slope of this functional representation) does not vary with respect to temperature. As previously mentioned by Wadsö **[19]**, it would seem that heat transfer through calorimeters equipped with an insulated sidewall (such as the QAB calorimeter) primarily takes place via conduction, whereas transfer with Langavant-type calorimeters mainly occurs, as indicated by Alègre **[5]**, through radiation, thus making these latter calorimeters temperature-dependent.

In reality, flux deviations relative to the regression line, as magnified in **Figure 15**, show a nonlinearity whose shape (in this figure) has been smoothed by a second-degree polynomial. The effects of radiation on heat transfer are nonetheless visible at this scale. A similar nonlinearity has been found for a set of calibration curves from various QAB calorimeters.

For the sake of accuracy, when determining and using α, the calibration protocol for Langavant-type calorimeters (Standard NF EN 196-9) is selected for the QAB calorimeters. The heat loss coefficient, α, is calculated for each of the four temperature plateaus (power divided by θ). Coefficients *a* and *b* are obtained by means of linear regression for α/θ.

Figure 16 indicates the influence of the associated heat conduction coefficient, which is considered to either vary with temperature or remain constant during heat release in a QAB calorimeter test. This deviation is observed to stay small (on the order of 3%).

Figure 16
Heat release of a conventional concrete mix used on engineering structures. The data have been analyzed with a heat loss coefficient that either varies with temperature or remains constant (see *Figs 14 and 15). These two types of heat loss coefficients were generated from the same calorimeter calibration dataset (featuring 4 temperature plateaus).*

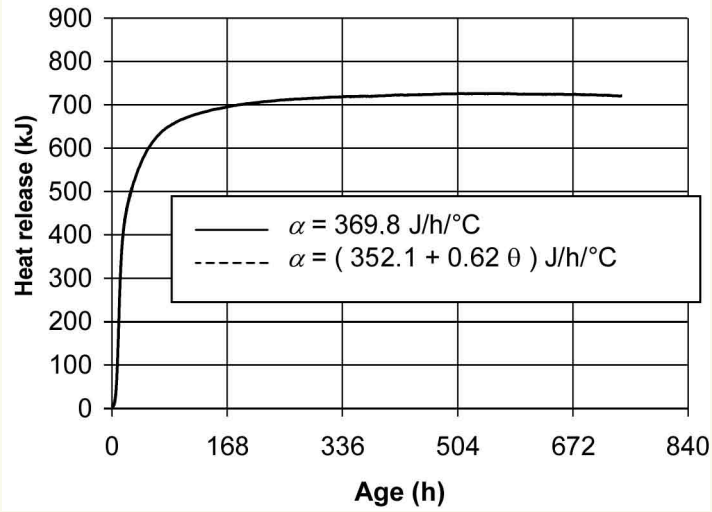

In summary, heat loss through the sidewalls of a QAB calorimeter mainly involves conduction. The little amount of radiation contributing to this heat transfer makes the heat conduction coefficient response slightly parabolic. The interpretation of heat release results from QAB calorimeter tests is not very sensitive to the choice of heat loss coefficient (i.e. constant vs. proportional to temperature). In contrast and out of concern for accuracy and homogeneity relative to Langavant calorimeter calibration procedures, it is preferable to introduce 4 temperature thresholds in order to determine a temperature-based heat loss coefficient, as proposed in Standard NF EN 196-9.

Determination of calorimeter heat capacity

Determining the calorimeter heat capacity (C_{cal}) consists of measuring the temperature drop once the current has stopped circulating following the last threshold (in other words, when the Joule effect heat source falls to 0). The calculation proceeds by assuming that the heat loss coefficient (α) and heat capacity of the reference cylinder (C_R) are both known. C_{cal} is the difference between total heat capacity (C_{tot}) and C_R. The focus then turns to determining C_{tot}.

Once the current has been shut off, heat loss in both the calorimeter and reference cylinder will equal, at every point in time, the losses incurred through the calorimeter sidewalls (as the product of flux α θ multiplied by time interval dt). This equation is written as follows:

$$-C_{tot}\,d\theta = (a + b\,\theta)\,\theta\,dt \qquad (14)$$

The solution to this differential equation (Standard NF EN 196-9) yields:

$$C_{tot} = \frac{a\,t_d}{\mathrm{Log}\left(\frac{\theta_0\ \alpha_t}{\theta_t\ \alpha_0}\right)} \qquad (15)$$

with:

t_d = time elapsed since shutting off the resistance power supply of the reference cylinder,

θ_0 = heating at time 0,

α_0 = heat loss coefficient at time 0 (for $\theta = \theta_0$),

θ_t = heating at time t_d,

α_t = heat loss coefficient at time t_d (for $\theta = \theta_t$).

Note: The numerator in the current version of Standard NF EN 196-9 is erroneous, appearing as α t_d instead of $a\ t_d$.

Temperature measurements are selected for 24, 26, 28 and 30 hours. At these times, the total capacity is calculated. An average of the 4 values obtained can then be calculated, with the heat capacity of the reference cylinder being subtracted out so as to leave the heat capacity of the empty calorimeter.

For the active calorimeter under study herein (no. 5), C_{tot} equals 16,751 J/°C on average and C_{cal} amounts to 3,266 J/°C (with C_{alu} = 13,485 J/°C).

Note: In reality, the calorimeter heat capacity calculation is affected by a bias stemming from the fact that calorimeter temperature is not homogeneous; instead, it varies between the value θ to the outside temperature value according to a slightly nonlinear profile **[8]**. This nonlinear trend however does not affect the heat of hydration estimation since the temperature profile in the calorimeter during the QAB test resembles the calibration profile.

UNCERTAINTY IN DETERMINING HEAT RELEASE

If q_∞ is to be found experimentally, then the test would need to be stopped once θ moves below its expanded uncertainty. Let u_a and u_c be the standard uncertainties of temperature measurements in the active and control calorimeters respectively, then the expanded uncertainty on θ (with an expansion factor of $k = 2$) is given by:

$$U_\theta = 2\sqrt{u_a^{\,2} + u_t^{\,2}} \qquad (16)$$

As an example, let's take a standard uncertainty on the order of 0.1°C. Under these conditions, U_θ equals 0.3°C.

Uncertainty in the determination of $q(t)$, according to Equation (1), depends on the elementary standard uncertainties of each term in this equation. To derive this result, a number of numerical calculations have been applied to a real-world case (using the conventional concrete described in **Table 2**).

Table 2
Composition of the concrete tested in the QAB calorimeter.

Components	Mass (in kg/m³)
CEM I 52.5 N PMES CP2	340
Bernières 0/4 sand	739.45
Bernières 8/22 gravel	1,072.1
Total water	184.22

During an initial step, the most comprehensive inventory possible **(see Table 3)** of elementary standard uncertainties, u_{xi}, is built (with Equation **(1)** being detailed to a point of deriving each parameter involved in the determination). In a subsequent step, the sensitivity, λ_i, of $q(t)$ with small variations, Δx_i, on each of these parameters is calculated numerically, i.e.

$$\lambda_i = \frac{\Delta q(t)}{\Delta x_i} \qquad (17)$$

Lastly, the standard uncertainty on the heat release determination can be calculated from the following expression **[20]**:

$$u_{q(t)} = \sqrt{\sum_i (u_{xi}\ \lambda_i)^2 + 2\sum_{i \neq j} \rho_{ij} \left(u_{xi}\ \lambda_i\right)\left(u_{xj}\ \lambda_j\right)} \qquad (18)$$

where ρ_{ij} is the correlation coefficient between variables x_i and x_j. This coefficient is considered to assume a value of 0, 1 or –1. Should these variables be independent, then $\rho = 0$ and the expression for uncertainty on the heat release can be simplified to: $u_{q(t)} = \sqrt{\sum_i (u_{xi}\ \lambda_i)^2}$.

In this inventory of elementary uncertainties, all mass values are considered as independent. Mix components are weighed separately, and each weighing exerts no influence on the subsequent weighing. The standard uncertainties of these weight recordings for a given concrete mix (10 to 30 liters) are then transposed into standard uncertainties on the quantities present in the specimen (6.4 liters) contained inside the calorimeter. The mass recording of concrete in the specimen is also independent of the other recordings. This mass of concrete poured into the mold allows retrieving the masses of components actually present in the specimen through mass proportions found in the concrete formulation.

The uncertainties **(Table 3)** on coefficients stemming from the calibration (C_{cal}, α) step are provided in the calorimeter calibration report.

The concrete specimen heat capacity can be calculated as shown in Standard NF EN 196-9, using conventional terms, by means of the following expression:

$$C_{concrete} = 800\ m_s + 3800\ m_e \qquad (19)$$

Table 3
Standard uncertainties u_{xi} of parameters x_i exerting an influence on the calculation of q(t).

Variable x_i	Nominal value	u_{xi}	Units
Mass of the empty mold	0.346	0.0002	kg
Mass of the filled mold	15.262	0.005	kg
Cement mass	2.171	0.005	kg
Water mass	1.176	0.0002	kg
Sand mass	4.722	0.005	kg
Gravel mass	6.846	0.005	kg
C_{cal}	3 266	12	J/°C
α	369.8	3.2	J/°C/h
Solid specific heat capacity	800	40	J/°C/kg
Liquid specific heat capacity	3 800	190	J/°C/kg
Concrete T	variable	0.1	°C
Control specimen T	variable	0.1	°C

whereby 800 and 3800 are respectively the specific heat capacities of the solid components and water, in J/°C/kg.

m_s and m_e are the masses of solid components and water, in kg. The solid mass equals the sum of sand, gravel and cement masses.

In this expression, the uncertainties on masses are known, while uncertainties on the specific heat capacities are not listed in the Standard and moreover their values are not explained.

A number of researchers have offered some indications on this topic **[4, 11, 14, 15, 20]**. When the concrete is fresh, specimen heat capacity equals the sum of heat capacities for each component. When specimen concrete has hardened, its heat capacity tends to increase with temperature and decrease with water content (as maturity advances). These two phenomena nearly offset one another, with on the whole a slight increase (0.5% to 2.5% depending on type of binder). It is readily recognized that the heat capacity calculation for fresh concrete accurately reflects the average value for concrete during setting and hardening. For semi-adiabatic tests, temperature increases are not as significant as those recorded during adiabatic tests; this approach is capable of overestimating the average heat capacity value of concrete (with, as a corollary, the temperature rise of concrete being underestimated). For this reason, AFNOR (AFN88) recommends introducing a lower specific heat capacity value for water (i.e. 3,800 instead of 4,180 J/°C/kg).

The specific heat capacity value for solid components has also been averaged, taking into account both aggregates and cement, given that the individual values are not straightforward to determine **[14]**: they vary between 710 and 890 J/°C/kg depending on the type of solid (**Table 4**). An average value of 800 J/°C/kg is considered acceptable.

Table 4
Specific heat capacities of concrete components at 20°C [4, 20].

Components	Specific heat capacity (in J/°C/kg)
Aggregates and fine-grained silica	730
Aggregates and fine-grained limestone	840
Dolomite aggregates	890
Anhydrous cement	760
Silica fume	730
Fly ash	730
Free water	4 190
Bound water	3 800

Figure 17
Proportion of elementary uncertainties vs. concrete age.

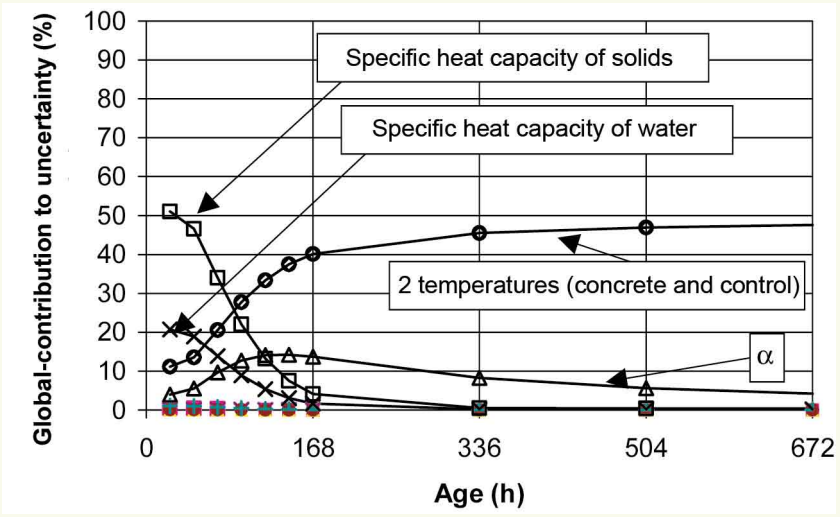

In definitive terms, given a lack of greater precision, the standard uncertainty adopted for these specific heat capacities is set equal to 5% of their nominal value **(Table 3)**, or 10% for expanded uncertainty with an expansion factor of 2.

For the purpose of visualizing the relative impact of each parameter on the heat release calculation, a comparison is drawn of the $\sqrt{(u_{xi}\ \lambda_i)^2}$ expressions, which are considered as the indicators of elementary uncertainties **(Fig. 17)**.

It is seen that during the first week of the test, uncertainties relative to specific heat capacity values capture the greatest share, followed by uncertainties on temperature measurements and then uncertainties on heat loss coefficients. It might be possible to improve the accuracy of these specific heat capacities, but it would not be very realistic to assume that temperature measurement accuracy could be improved. The other variables account for just a slight, and negligible, contribution.

Accuracy on the order of 0.1°C is not entirely infeasible, although such a goal would justify the introduction of platinum probes, along with a Kelvin (4-wire) assembly and a highly meticulous calibration process. In addition to these precautions, sheathed probes would need to be used in a stainless steel sleeve of sufficient length (16 to 20 cm) so that no water entry could be suspected, especially at the time of calibration.

Accuracy on the heat loss coefficient is no simpler to improve. It is also noteworthy that the calorimeter heat capacity determination exerts a negligible impact on the assessment of uncertainties, which correlates well with the observation of a determination protocol taking place under non-homogeneous conditions (*see the section entitled* "Determination of calorimeter heat capacity").

Since temperature measurement accuracy is the most critical parameter after one week of testing, it makes sense to examine how this accuracy is correlated with uncertainty on the heat release calculation; such an investigation requires successively applying various values for the standard uncertainty (0.05-0.3°C) on temperature measurements **(Fig. 18)**, as an input to calculating the uncertainty on $q(t)$. This standard uncertainty range corresponds to an interval from 0.1° to 0.6°C for expanded uncertainties (with the expansion coefficient[3], k, equal to 2).

On this diagram, the uncertainty on heat released is seen not to behave like a constant; it begins at 5% and then declines for a week (inaccuracy on specific heat capacities), followed by a nearly linear increase thereafter as a result of inaccuracy on temperature measurements. By setting a 10% threshold for relative uncertainty on the heat released (expansion factor = 2), the expanded uncertainty for temperature measurements must be less than 0.2°C. This limit leads to an interval like the one illustrated in **Figure 19**, which also includes uncertainties on both specific heat capacities and

[3]*When k = 2, the probability that values lie outside the expanded uncertainty interval equals 0.05.*

Figure 18
Variation in relative uncertainties on the heat release measurement as standard uncertainty on the temperature measurements varies. In this context, relative uncertainty is defined as the expanded uncertainty of q(t) divided by the value q(t).

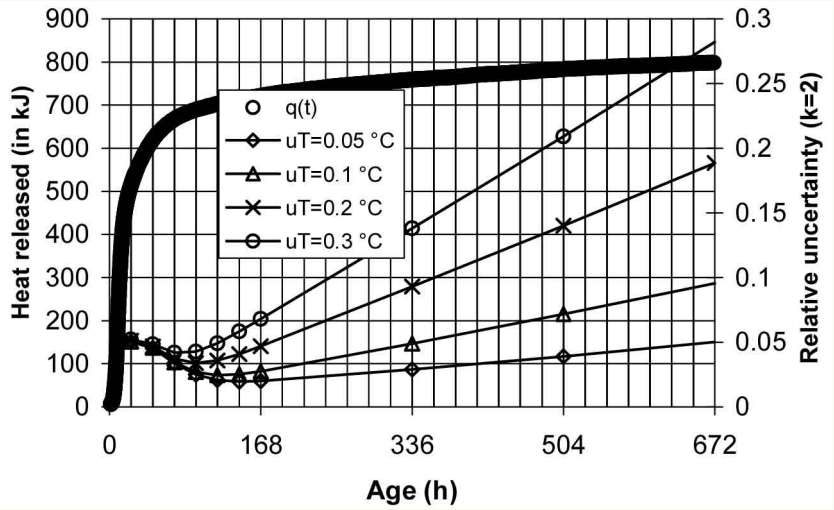

Figure 19
Interval covering potentially 95% of the calculated values using the dataset in Table 3.

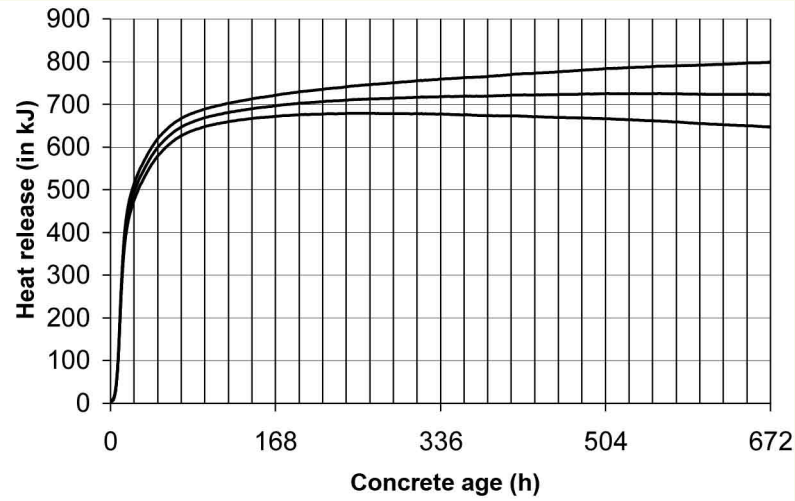

the heat loss coefficient. For this example, extending measurements beyond two weeks is clearly of no utility[4].

This approach has not been applied to the other quantities capable of being determined (i.e. heat flux, adiabatic temperature rise, chemical affinity).

CONCLUSION

The test to determine the heat of hydration of a concrete specimen using the QAB calorimeter has been analyzed in detail herein. This analysis has served to validate the draft test method, which has been shaped along the lines of the standard on cement and mortar calorimetry.

It would appear that heat is transferred through this type of calorimeter primarily by conduction. A very small share of radiation leads to processing the calibration data, for the sake of accuracy, as is the case with Langavant bottles, whose heat is mainly lost due to radiation.

With the aim of improving accuracy, temperature measurements need to be carried out on an active specimen placed in a first calorimeter at the same time as an inert concrete specimen is held in a second, matching calorimeter. Platinum resistance probes are also recommended as a means of achieving the required accuracy levels.

[4] *It can nonetheless be advised not to stop testing too early since direct analyses often lead to difficulties.*

Calibration uncertainties on QAB calorimeters exert a secondary influence with respect to the accuracy required for temperature measurements performed on both the concrete test specimen and control specimen. Another way to improve uncertainty on the heat release measurement would be to develop greater knowledge of the specific heat capacity of solid components and water vs. progress in the hydration reaction.

Ambient temperature fluctuations over a ±2°C range only cause negligible temperature deviations between the active calorimeter and control calorimeter.

Despite being advised to only supply the platinum resistance temperature probes while measurements are being recorded, these probes can still be supplied on a continuous basis provided power supply current is on the order of 1 mA. Beyond this value, the quantity of heat applied to the specimen becomes significant.

This estimation of heat release measurement uncertainty in a QAB calorimeter does not take into account reproducibility of the operating procedure. Quantifying these uncertainties can only be fully accomplished upon completion of a cross-testing campaign.

REFERENCES

1 **André J. L.**, **Saintilan R.**, « Étalonnage des caissons QAB », *BLPC*, n° 278, **2010**, pp. 43-48.

2 **Acker P.**, Comportement mécanique du béton : apports de l'approche physico-chimique, Thèse de l'Ecole nationale des ponts et chaussées, Paris, Rapport de Recherche LPC 152, **1988**.

3 **Acker P.**, **Chauvin J. J.**, Essais calorimétriques sur béton : banque de données, Paris : *LCPC*, Bordeaux : CETE du sud-ouest, rapport interne, **1990**, 63 pages.

4 **Acker P.**, **Torrenti J. M.**, **Ulm F. J.**, Comportement du béton au jeune âge, collection Mécanique et Ingénierie des Matériaux, Hermès Sciences, **2004**, 188 p.

5 **Alègre R.**, La calorimétrie des ciments au CERILH, *Publication technique n° 119*, **1961**, 164 pages.

6 **Boulay C.**, **André J. L.**, **Torrenti J. M.**, « Projet de mode opératoire pour la détermination de la chaleur dégagée lors de l'hydratation du ciment d'un béton placé dans un calorimètre Quasi Adiabatique pour Bétons (QAB) », *BLPC*, n° 278, **2010**, pp. 37-42.

7 **Briffaut M.**, **Benboudjema F.**, **Torrenti J. M.**, **Nahas G.**, « Etude expérimentale d'un béton au jeune âge et modélisation macroscopique associée », Congrès français de Mécanique, Marseille, **2009**.

8 **Briffaut M.**, **Benboudjema F.**, **Nahas G.**, **Torrenti J. M.**, Simulations numériques des essais semi-adiabatique QAB et Langavant et comparaison aux résultats de mesures expérimentales, *BLPC*, n° 278, **2010**, pp. 5-18.

9 **Buffo-Lacarrière L.**, Prévision et évaluation de la fissuration précoce des ouvrages en béton. Thèse de l'Institut National des Sciences Appliquées de Toulouse, **2007**.

10 **D'Aloia L.**, Détermination de l'énergie d'activation apparente du béton dans le cadre de l'application de la méthode du temps équivalent à la prévision de la résistance en compression au jeune âge : approches expérimentales mécanique et calorimétrique, simulations numériques, thèse de l'INSA de Lyon, **2 mars 1998**, 278 p.

11 **De Larrard F.**, *Structures granulaires et formulation des bétons*, Collection Études et Recherches des Laboratoires des Ponts et Chaussées, OA 34, **avril 2000**, 409 p.

12 **De Schutter G.**, **Taerwe L.**, General hydration model for portland cement and blast furnace slag cement, *Cement and Concrete Research*, Vol. 25, n° 3, **1995**, pp. 593-604.

13 **LCPC**, Résistance du béton dans l'ouvrage – La maturométrie, Guide technique LCPC, IREX Calibé, Paris, **mars 2003**.

14 **Hamfler H.**, **Röhling S.**, **Van Breugel K.**, "Methods for calculating temperatures in hardening concrete structures", RILEM TC119TCE, Chapter 6, draft 4, Rilem, **1993**.

15 **Jolicœur C.**, Étude calorimétrique de l'hydratation du ciment : détermination de l'énergie d'activation, rapport interne, Université de Sherbrooke, **1994**.

16 **Lackner R.**, **Pichler C.**, **Mang H. A.**, Thermo-chemomechanics of cement-based materials at finer scales of observation: Application to hybrid analyses of shotcrete tunnel linings, in: *Engineering Structures under Extreme Conditions - Multi-Physics and Multi-Scale Computer Models in Non-Linear Analysis and Optimal Design*, A. Ibrahimbegovic, B. Brank (Hrg.); IOS Press, **2005**, ISBN: 1 58603 479 0, pp. 170-199.

17 **Mounanga P.**, **Khelidj A.**, **Bastian G.**, Experimental study and modelling approaches for the thermal conductivity evolution of hydrating cement paste, *Advances in Cement Research*, vol.16, n° 3, **2004**, pp. 95-103.

18 **Ulm F.**, **Torrenti J. M.**, Modélisation du comportement du béton au jeune âge, In *Comportement du béton au jeune âge* (Traité MIM, série Matériaux de construction), sous la direction de P. Acker, J.M. Torrenti et F. Ulm, **2004**, éditions Hermès.

19 **Wadsö L.**, An experimental comparison between isothermal calorimetry, semi-adiabatic calorimetry and solution calorimetry for the study of cement hydration, Nordtest report TR522, **2003**, March, 42 p.

20 **Waller V.**, Relations entre composition des bétons, exothermie en cours de prise et résistance en compression, Collection Études et Recherches des Laboratoires des Ponts et Chaussées, OA35, mai **2000**, 317 p.